Published in final edited form as:

Neuroimage. 2021 September ; 238: 118205. doi:10.1016/j.neuroimage.2021.118205.

Fronto-subthalamic phase synchronization and cross-frequency coupling during conflict processing

Ke Zeng[a], **Neil M. Drummond**[a], **Ayda Ghahremani**[a,b], **Utpal Saha**[a], **Suneil K. Kalia**[a,c], **Mojgan Hodaie**[a,c], **Andres M. Lozano**[a,c], **Adam R. Aron**[d], **Robert Chen**[a,e,f,*]

[a]Krembil Research Institute, University Health Network, Toronto, Ontario, Canada

[b]School of Medicine, Stanford University, Stanford, California, USA

[c]Division of Neurosurgery, Department of Surgery, University of Toronto, Toronto, Ontario, Canada

[d]Department of Psychology, University of California San Diego, San Diego, California, USA

[e]Division of Neurology, Department of Medicine, University of Toronto, Toronto, Ontario, Canada

[f]Edmond J. Safra Program in Parkinson's Disease, University Health Network, Toronto, Ontario, Canada

Abstract

Growing evidence suggests that both the medial prefrontal cortex (mPFC) and the subthalamic nucleus (STN) play crucial roles in conflict processing, but how these two structures coordinate their activities remains poorly understood. We simultaneously recorded electroencephalogram from the mPFC and local field potentials from the STN using deep brain stimulation electrodes in 13 Parkinson's disease patients while they performed a Stroop task. Both mPFC and STN showed significant increases in theta activities (2–8 Hz) in incongruent trials compared to the congruent trials. The theta activity in incongruent trials also demonstrated significantly increased phase synchronization between mPFC and STN. Furthermore, the amplitude of gamma oscillation was modulated by the phase of theta activity at the STN in incongruent trials. Such theta-gamma phase-amplitude coupling (PAC) was much stronger for incongruent trials with faster reaction times than those with slower reaction times. Elevated theta-gamma PAC in the STN provides a novel mechanism by which the STN may operationalize its proposed "hold-your-horses" role. The co-occurrence of mPFC-STN theta phase synchronization and STN theta-gamma PAC reflects a neural substrate for fronto-subthalamic communication during conflict processing. More broadly, it may be a general mechanism for neuronal interactions in the cortico-basal ganglia circuits via a combination of long-range, within-frequency phase synchronization and local cross-frequency PAC.

*Corresponding author. robert.chen@uhn.ca (R. Chen).

Declaration of Competing of Interest

The authors declare no competing financial interests.

1. Introduction

The ability to avoid habitual responses is crucial to successfully navigate a complex and rapidly changing world. It is widely believed that the medial prefrontal cortex (mPFC)-basal ganglia system facilitates a more deliberative response process among multiple conflicting choices (Aron et al., 2016; DeLong, 1990; Mink, 1996). According to computational modeling of cortico-basal ganglia function in decision making (Frank et al., 2007), the mPFC is broadly implicated in determining which strategies and actions are most appropriate for the task at hand (Botvinick, 2007; Botvinick et al., 2004), and the STN is specifically thought to act as a brake on the cortico-basal ganglia system and buy more time until the optimal decision can be made (Rodriguez-Oroz et al., 2011; Zavala et al., 2015). Flexible conflict response thus requires the integration of information across spatially segregated mPFC-basal ganglia circuit. Anatomical and physiological studies demonstrate that the STN receives direct projections from the mPFC, involving a 'hyperdirect' pathway that can rapidly modulate cortico-basal ganglia processing (Aron et al., 2007; Chen et al., 2020). Although evidence supports this idea of a hyperdirect pathway, the neural mechanism underlying how these two brain regions communicate during conflict processing remains unclear.

Neural oscillatory activity in the STN has been found to be modulated in a wide range of temporal scales during cognitive control. Whereas gamma (> 30 Hz) band activity have been link to arousal, execution and cognitive load (Jenkinson et al., 2013; Wessel et al., 2016b), lower frequency oscillation (2–8 Hz, hereafter refer to as theta band) is mainly associated with goal-guided, top-down control of stimulus processing (Cavanagh et al., 2011; Herz et al., 2016). Cross-frequency coupling has been proposed to constitute a flexible mechanism for combining information across different temporal scales within local networks (Aru et al., 2015; Canolty and Knight, 2010; Hyafil et al., 2015). As a statistical dependence between the phase of low-frequency oscillation and the amplitude of high-frequency oscillation of brain activity, phase-amplitude coupling (PAC) is thought to operate through a physiologically plausible mechanism (Cardin et al., 2009). Since the first report of PAC in the human neocortex (Canolty et al., 2006), theta-gamma PAC has been extensively demonstrated as a mechanism for effective communication within human cortex and subcortical structures during cognitive processing (Cohen et al., 2009; Reinhart and Nguyen, 2019; Sweeney-Reed et al., 2014). In addition, the exaggerated coupling between the phase of the beta rhythm and the amplitude of broadband gamma activity in the motor cortex (De Hemptinne et al., 2015; Swann et al., 2015) and the STN (Lopez-Azcarate et al., 2010) have been revealed as potential pathophysiological features of Parkinson's disease (PD), and can be decoupled by therapeutic deep brain stimulation and dopaminergic medications. Hence, it can be hypothesized that gamma activity is modulated by the phase of theta activity locally within the STN during conflict processing.

In the mPFC-STN circuit, the STN has been proposed to serve as a downstream target for implementing the optimal strategy identified by mPFC during cognitive control (Zavala et al., 2018). Synchronized oscillations have been proposed as an effective way to integrate information across distant brain regions during cognition control (Fries, 2015). Activated neuronal groups coherently oscillate and such neural coherence represents a flexible and

effective communication at the timescale in which cognitive demands change (Womelsdorf et al., 2007). In support of this notion, concurrently elevated theta activity in mPFC and STN have been reported during conflict processing (Zavala et al., 2018, 2016), and importantly, the theta activity of the mPFC was shown to drive that of the STN (Zavala et al., 2014). Furthermore, high frequency DBS to the STN appears to disrupt the relationship between mPFC theta activity and reaction time in conflict conditions (Cavanagh et al., 2011), while 4 Hz (theta frequency) DBS to the STN seems to enhance mPFC theta activity and improve response inhibition (Kelley et al., 2018). These observations motivated the hypothesis that human mPFC and STN coordinate their function of conflict processing via long-range theta synchronization.

We hypothesize that the STN exhibits enhanced theta-gamma PAC and concurrently communicates with mPFC through theta synchronization during conflict processing. We simultaneous recorded frontal midline scalp electroencephalographic (EEG) and STN local field potentials (LFP) with deep brain stimulation electrodes from PD patients while they performed a Stroop task. Our results revealed fronto-subthalamic interactions via a combination of long-range, within-frequency phase synchronization and local cross-frequency PAC.

2. Materials and methods

2.1. Subjects

Thirteen PD patients (9 men, mean age = 60.4 years, range = 44–73 years) undergoing DBS surgeries were recruited. Patients provided written informed consent and the protocol was approved by the University Health Network (Toronto) Research Ethics Board. One patient was excluded from the analysis as he had excessive dyskinesia that affected the recordings, and another two patients were excluded because of artifacts in the local field potential data. The patients underwent bilateral implantation of quadripolar electrodes with 4 platinum-iridium contacts (numbered 0 to 3, Model 3387; Medtronic, Minneapolis, MN) in the STN, with the most ventral contact (contact 0) placed at the base of the STN. After the first surgery, DBS leads were externalized through the scalp, which enabled recordings the LFP in STN before the subcutaneous pulse generator was implanted in the second surgery. Patients were tested on medications to ensure task performance and motor functions were as normal as possible. More details on the patients and the surgical procedures can be found in a previous report that studied the same cohort of patients (Ghahremani et al., 2018).

2.2. Experimental procedure

Patients performed a Stroop task, in which they were required to verbalize the color but not the name of the word. A schematic of the task is shown in Fig. 1A. Each trial began with a black screen containing the word “READY” in the middle of the screen for 1 s to prepare the subjects. The imperative cues then appeared as any of “RED” “GREEN” “YELLOW” or “BLUE” written either with the ink of the same color (congruent trial) or with a different color (incongruent trial). The ratio between congruent and incongruent trials was 1:1. Subjects were instructed to speak the color of the word into a microphone as fast as

possible. After the response, a fixation cross was shown in the middle of the screen, and the interval between the response and the next trial was randomized between 3 to 5 s.

Before the Stroop task, the voice amplitude levels (root mean square power) of patients were gauged with the internal microphone of an Apple MacBook. Calibration was made to detect the voice onset of each patient, and reaction time (RT) was automatically calculated online using a custom-made script and Psychtoolbox sound recording system. The experiment started with a training block of 16 trials. The patients then completed a baseline block, consisting of 48 trials to obtain an initial estimate of RT for both congruent and incongruent conditions. Subsequently, the patients performed 5 test blocks (total of 240 trials), which contained four event-related DBS conditions, one in each trial (no stimulation, Ready period, Early response, and Late response). The results of event-related DBS have been reported (Ghahremani et al., 2018). The present study analyzed the no stimulation trials from the test blocks, resulting in 30 trials per condition (congruent / incongruent) per patient.

2.3. Electrophysiological recordings and pre-processing

Bilateral STN LFPs and scalp EEG were recorded at a sampling frequency of 5 kHz, filtered between 1 and 1,000Hz, and amplified using a SynAmp or SynAmp RT amplifier (Neuroscan Laboratories, El Paso, TX). LFPs were recorded from the DBS electrodes, and EEG was recorded from electrodes placed over (or close to if sutures had to be avoided) Fp1, Fz, Cz, C3, C4, P3, and P4 according to the international 10–20 system. Electrooculogram (EOG) was recorded to remove eye blink artefacts in subsequent data processing.

A rater checked the individual speech responses to exclude trials with noise, and only trials with clear speech responses were analyzed. All incorrect responses as well as any trials with reaction times >2 s (including no response trials) or <200 ms were discarded. For the remaining trials, those with reaction times that faster or slower than 3 SDs of the mean reaction time, or with clear artifact in either the EEG or LFP bipolar traces, were discarded. The mean (SD) number of trials per patient included were 27.8 (2.0) for congruent trials and 23.5 (4.2) for incongruent trials. Monopolar recordings were down-sampled to 1000 Hz, notch filtered at 60 Hz, and converted to a bipolar montage between adjacent contacts. Since event-related stimulation was applied unilaterally to the right STN and connection to the stimulator caused artifacts in the right STN recordings even when stimulation was not applied, we only analyzed LFP data from the left side which was free of artifacts. The adjacent contact pair (0–1, 1–2 or 2–3) with the highest beta (13–30 Hz) power in the left STN was chosen for further analysis as it has been shown to indicate the contacts most likely within the STN (Wessel et al., 2016a). Custom-written MATLAB scripts along with FieldTrip toolboxes were used to for data pre-processing (Oostenveld et al., 2011).

2.4. Spectral power analysis

Event-related potentials (ERPs) from stimulus (colored word) onset were first calculated by averaging the cue-aligned LFP/EEG signals across trials, and subtracted from each trial. The LFP/EEG signals were then re-aligned to the response and the following analyses were

response-aligned analysis. The ERPs of response were also removed by subtracting the average of the response-aligned LFP/EEG signals from each trial. For all time-frequency analyses, the time window of interest for each trial was from 1.2 s before the response to the response (t = −1.2 s to 0 s, relative to the response) and the frequency range was from 2 to 100 Hz. The baseline period consisted of the full second from the READY cue to the color word onset (Fig. 1A). A 2 s buffer on either side was used to eliminate edge artifacts. To obtain magnitude and instantaneous phase information in the frequency domain, STN LFPs and scalp EEG signals in each trial were convolved with Morlet wavelets. To make a tradeoff between time and frequency resolution, the ratio of frequency f and spectral resolution σ_f, that is f/σ_f, was set to a constant value 7, which is a standard value given the range of frequencies investigated here. For each frequency between 2 to 100 Hz in steps of 0.05 Hz, we calculated the product between the wavelets and bipolar LFP/EEG in steps of 10 ms, which was sufficient to address oscillatory dynamics for the current study. Time-frequency power estimates were extracted by calculating the squared magnitude of the complex wavelet-convolved data.

To assess the differences in induced spectral power between congruent and incongruent trials, the following approach was used. A mean time-frequency image for each trial type was calculated by averaging the spectrum power across trials. All time-frequency points were then normalized to the 1000 ms baseline period from the READY cue to the color word onset. This procedure produced one normalized spectrogram for the STN and one for the mPFC per trial type. Statistical differences between the power of congruent and incongruent trial types were assessed by cluster-based permutation tests (Maris and Oostenveld, 2007). For each time-frequency pixel, a samplewise paired t value was estimated by comparing incongruent and congruent condition, and only data points with p value lower than a threshold of 0.05 were considered and clustered. The trials conditions for each subject were then randomly shuffled 1,000 times to yield the permutation distribution. Based on this distribution, the clusters were considered significant with $p < 0.05$ (2-tailed). To generate the theta band power time series, the same procedure was used, but the values across 2–8 Hz were first averaged before any calculation.

2.5. Inter-site phase coherence analysis

The STN-cortex phase synchronization was measured by wavelet phase coherence (Lachaux et al., 2002; Nolte et al., 2004). The inter-site phase coherence values (Coh) at (t, f) was estimated by projecting the phase difference between STN and cortex at (t, f) for each trial onto a complex plane and averaging across trials, as follows:

$$Coh(t,f) = \left| \frac{1}{N} \sum_{n=1}^{N} e^{i*\left(\theta_{t,f}^{LFP_n} - \theta_{t,f}^{EEG_n}\right)} \right|$$

where N was the total number of trials, $\theta_{t,f}^{LFP_n}$ and $\theta_{t,f}^{EEG_n}$ were instantaneous phase of LFP and EEG in the nth trial at point (t, f). The range of Coh(t, f) is from 0 to 1, where 0 indicates random phase differences between STN and cortex at point (t, f) across trials, and 1 indicates identical phase differences between STN and cortex at point (t, f) across trials.

The phase coherences between mPFC and STN signals were calculated separately for congruent and incongruent trials and normalized by determining the percentage change relative to the "baseline" coherence recorded from the READY cue to the color word onset. Statistical significance was determined using permutation testing as outlined above. To test whether the synchronization was specific between the mPFC and the STN, phase coherence between bipolar LFP and P3-C3 was also calculated for comparison. Bipolar EEG at P3-C3 was chosen since LFP was recorded from the left STN.

2.6. Inter-trial phase clustering analysis

To analyze phase consistency (also referred to as phase-resetting) across trials during conflict processing, inter-trial phase clustering (ITPC) was calculated for mPFC EEG and STN LFP in this study. ITPC(t, f) was estimated by projecting the instantaneous phase for each trial onto a complex plane and averaging across trials (Cohen and Gulbinaite, 2014; Daume et al., 2021; Vinck et al., 2010), as follows:

$$ITPC(t, f) = \left| \frac{1}{N} \sum_{n=1}^{N} e^{i * \theta_{t,f}^{n}} \right|$$

where N was the total number of trials, and $\theta_{t,f}^{n}$ was the instantaneous phase of LFP/EEG in the n th trial at point (t, f), which was extracted from the wavelet transform data. ITPC(t, f) varies from 0 to 1, where 0 means random phases at point (t, f) across trials, and 1 means identical phase values at point (t, f) across trials. The time-frequency ITPC were calculated for each trial type, and normalized to a 1000 ms baseline period recorded from the READY cue to the color word onset. Statistical differences between the ITPC of congruent and incongruent trial types were also assessed by cluster-based permutation tests (Maris and Oostenveld, 2007), and the statistical analysis procedure was similar as that in spectral power.

2.7. Phase amplitude coupling analysis

PAC was calculated for a variety of frequency combinations: the phase of frequencies between 2 and 16 Hz (in steps of 0.25 Hz; termed "phase frequencies") and amplitudes of frequencies between 32 and 96 Hz (in steps of 1 Hz; termed "amplitude frequencies"). The time window of interest was between imperative cues and the subjects' response time (reaction time period) of each trial. We filtered the time window of interest plus additional "buffer" windows of 1000 ms before and after that window of interest for bipolar LFP and EEG signals using Morlet wavelets for the slow oscillation (bandwidth, 0.5 Hz) and the fast oscillation (bandwidth, 1 Hz). The instantaneous phase of the slow frequencies and the amplitude of the fast frequencies were extracted using Hilbert transformation. The time windows of interest across all trials were then concatenated into one vector in congruent and incongruent condition. Thereafter, the modulation index (MI) for each pair of frequencies was computed using the Kullback-Leibler based method (Tort et al., 2008, 2009). In brief, the low-frequency phases were binned into 20° intervals (18 bins), and amplitudes of the high-frequency activity were assigned to each phase bin of the low-frequency activity. The mean amplitude for each bin was then calculated and normalized by the sum of the mean

amplitudes for all bins, creating a distribution similar to a probability distribution. If no PAC was evident, the corresponding amplitude distribution across the bins was uniform. The MIs were derived of the Kullback-Leibler divergence between the amplitude distribution and a uniform distribution. This procedure was repeated for all combinations of phase and amplitude frequencies and a comodulogram can be obtained in the final. Grid points with high MI values reflect a higher degree of PAC as compared with grid points with lower MI values. PAC was calculated using custom routines in Python, incorporating functions from the Tensorpac toolbox (https://etiennecmb.github.io/tensorpac/).

PACs were calculated separately for the mPFC EEG and STN LFP, and long-range PACs was also calculated cross mPFC (phase) and STN (amplitude) to test whether mPFC activity modulated STN activity directly during conflict processing. Theta-gamma PAC value was derived by averaging MI values over the theta band range (2–8 Hz) for the phase frequency, and the gamma range (32–64 Hz) for the amplitude frequency, for each trial type in each subject. Group statistics were performed to compare theta-gamma PAC value in congruent and incongruent trials, and a nonparametric Wilcoxon signed rank (paired) test was used. In addition, correlations between theta power and theta-gamma PAC were calculated to determine whether the theta-gamma PAC depended on theta power.

To test whether trials with faster reaction time had higher theta-gamma PAC during conflict processing, each successful incongruent trial was classified as either fast or slow reaction time based on a median split within each subject. The same procedure of PAC calculation and group statistics were repeated for fast and slow incongruent trials. We also performed a parallel analysis of group differences in PAC after converting each subject's PAC values to a z-score by a surrogate-data method (Tort et al., 2008). The z-score was calculated as follows: 1) generate 200 surrogate phase signals based on shifting the phase signal by a random value relative to the amplitude signal, 2) estimate the PAC for each pair of surrogate phases and amplitude signals, resulting in surrogate distribution, 3) calculate the z-score of raw PAC based on the surrogate distribution. The normalization based on surrogate-data method can remove some spurious coupling such as those with a consistent periodic profile or electrical artifact.

2.8. Data availability

The data and code that support the findings of this study are available from the corresponding author, upon reasonable request.

3. Results

3.1. Spectral power changes in STN and mPFC

As reported in our previous work (Ghahremani et al., 2018), behavior analysis showed that patients were significantly slower in incongruent trials relative to congruent trials (Fig. 1*B*, 1.15 ± 0.14 s vs 0.92 ± 0.12 s; $p < 0.001$, paired t test) and show a significantly higher error rate during conflict (10.1 ± 6.2% vs 2.5 ± 3.3 %, $p < 0.01$, paired t test). In addition, we previously demonstrated increased theta power in the STN before the response for the incongruent trials compared to the congruent trials (Ghahremani et al., 2018). Here, we

extended the spectral power analysis to the mPFC and examined the relationship between oscillatory activities in the mPFC and STN.

The response-aligned STN LFP spectral power for congruent and incongruent trials are illustrated in Fig. 2A and 2B. Fig. 2*C* shows the time-frequency points when LFP power was significantly different between the two trial types, and reveals higher pre-response, conflict-related activity in the theta band ($p < 0.05$, permutation test). Over the time window from −0.83 to −0.41 s in Fig. 2*D*, the mean theta power in STN was significantly higher for incongruent trials (33.9 ± 6.2%) than congruent trials (−1.1 ± 4.9%). For mPFC (Fz-Cz), the spectral power for congruent and incongruent trials are illustrated in Fig. 2E and 2F. We also found significant conflict-related difference in theta power ($p < 0.05$, Fig. 2G). Over the time window from −0.76 to −0.35 s in Fig. 2H, the mean theta power in mPFC was significantly higher for incongruent trials (74.5 ± 29.1%) than congruent trials (−15.1 ± 16.2%).

3.2. Theta phase synchronization between STN and mPFC

The response-aligned mPFC-STN phase coherence for congruent and incongruent trials are illustrated in Fig. 3A and 3B. Fig. 3C shows the time-frequency points where phase coherence values were significantly different between the two trial types, and reveals higher phase coherence in the theta band for the incongruent trials ($p < 0.05$, permutation test). To explore this phenomenon further, the average mPFC-STN theta phase coherence time series are plotted in Fig. 3D. Over the time window from −0.66 to −0.18 s in Fig. 3D, the incongruent trials had significantly higher change in theta phase coherence (58.6 ± 16.7%) than that in congruent trials (5.3 ± 5.9%).

As a control, the response-aligned PPC-STN phase coherence for congruent and incongruent trials are illustrated in Fig. 3E and 3F. No significant difference between trial types was observed in the time-frequency space of PPC-STN phase coherence (Fig. 3G) or continuous time series of PPC-STN theta phase coherence (Fig. 3H). These results suggested that the conflict related theta phase coherence was specific to the frontal-STN circuit. In addition, the inter-trial phase clustering was analyzed for mPFC EEG and STN LFP and illustrated in Fig. 4. In contrast to the conflicted related increase in mPFC-STN theta phase coherence, there was no significant difference in response-aligned inter-trial phase clustering between incongruent trials and congruent trials at STN or mPFC. Hence, changes in inter-site phase coherence can occur without changes in inter-trial phase clustering at either site.

3.3. Theta-gamma coupling in STN

PAC was calculated for STN and mPFC signals during the reaction time period. Group mean PAC comodulograms in STN for congruent and incongruent trials are shown in Fig. 5A and 5B. Theta-gamma PAC in STN for incongruent trials was significantly stronger than congruent trials (Fig. 5C and 5D, 2-tailed, Wilcoxon sign rank test, $p = 0.023$). This result was also significant if individual subject PAC were first converted to a z-score prior to group statistics (Fig. 5E and 5F, $p = 0.01$). However, such theta-gamma PAC difference between trial types was not observed at mPFC ($p = 0.507$). In addition, there was no significant difference in mPFC-STN theta-gamma PAC between congruent and incongruent trials (p

= 0.878). STN theta power and STN theta-gamma PAC did not correlate in either the congruent (p = 0.33) or incongruent trials (p = 0.21).

To determine whether theta-gamma coupling in STN was stronger for the incongruent trials with faster reaction times, we repeated the phase-amplitude coupling analysis for the incongruent trials with median split into fast and slow halves. Fig. 6A and 6B demonstrate the group mean PAC comodulograms for the fast and slow incongruent trials. Theta-gamma coupling in fast incongruent was significantly higher than that in slow incongruent trials (Fig. 6C and 6D, 2-tailed, paired Wilcoxon sign rank test, p = 0.009). This result was also significant if individual subject PAC were first converted to z-scores (Fig. 6E and 6F, p = 0.036).

4. Discussion

We previously reported elevated theta power (2–8 Hz) during conflict processing in the STN (Ghahremani et al., 2018). The present analyses showed that conflict processing was associated with concurrently increased theta activity in the STN and mPFC. Moreover, the theta activity at the two sites demonstrated increased phase synchronization, which revealed significant fronto-subthalamic interactions during conflict processing. The STN also exhibited enhanced theta-gamma coupling in the incongruent trials, and the incongruent trials with shorter reaction times demonstrated stronger theta-gamma coupling.

4.1. Role of fronto-subthalamic theta activity

Theta oscillations have been considered as the potential “language” by which mPFC communicates with other brain structures for cognitive control (Cavanagh and Frank, 2014; Narayanan et al., 2013). The mPFC theta power was previous found to be correlated with reaction time during conflict scenarios, and such correlation was abolished by high-frequency STN-DBS (Cavanagh et al., 2011). In line with previous conflict-related studies (Brittain et al., 2012; Zavala et al., 2018), the elevated theta power in mPFC was accompanied by a similar increase of theta activity in STN during conflict processing. The STN theta activity has been considered a mechanism by which STN dynamically adjusts the decision threshold during response conflict (Cavanagh et al., 2011; Herz et al., 2016). As such, our results add to a growing body of evidence supporting computational based hypotheses that the mPFC and STN play crucial roles in decision making (Frank et al., 2007).

4.2. Fronto-subthalamic interaction through theta phase synchronization

The elevated theta power in mPFC and STN during conflict was accompanied by an increase in mPFC-STN theta phase coherence. Importantly, this coherence was specific to the fronto-subthalamic circuit. Brain processing depends on the interactions between neuronal groups, and synchronization between two groups of neurons can facilitate interactions between them (Fries, 2005, 2015). The STN theta activity has been shown to be driven by the mPFC theta activity with a gradually adapting dot motion task (Zavala et al., 2014). Our findings regarding conflict related mPFC-STN theta phase coherence provide direct evidence of such interaction in rapid onset conflict situations. The PFC has been associated with top-down

control and it has been suggested that increased synchronizations between the PFC and other areas reflect such control processes (Cohen, 2014; Helfrich and Knight, 2016). Our results of enhanced theta phase synchronization between the mPFC and STN during conflict processing support this idea.

Neural information may be encoded using the phases of ongoing oscillations, and phase-resetting also can be considered as a tool of information transmission (Canavier, 2015). However, in contrast to the theta phase coherence between mPFC and STN, we did not observe conflict related differences in inter-trial phase clustering in either mPFC EEG or STN LFP. This suggests that phase difference between two signals did not depend on the inter-trial phase clustering in either signal, and changes in inter-site phase coherence can occur without changes in inter-trial phase clustering at either site. Our data also suggested that it is the relative phase difference between mPFC and STN activities (phase coherence) that supports fronto-subthalamic interaction during conflict processing, but not the absolute phase in each structure (inter-trial phase clustering). This finding may also help to explain previous contradictory results that some studies found conflict related differences in inter-trial phase clustering at mPFC (Cohen and Cavanagh, 2011) and STN (Zavala et al., 2013), but others did not (Cavanagh et al., 2012; Zavala et al., 2016).

4.3. Conflict processing is associated with enhanced PAC in the STN

Our finding of enhanced theta-gamma PAC in STN strongly support the view that PAC provides a mechanism for effective communication during cognitive processing in humans (Canolty and Knight, 2010; Hyafil et al., 2015). Previous animal studies have linked theta-gamma coupling in cortico-basal ganglia network to both basic motor tasks (von Nicolai et al., 2014) and advance cognitive tasks (Tort et al., 2008). Our study extended these findings to the human cortico-basal ganglia network. We did not observe conflict related increased PAC in mPFC, though a previous study demonstrated PAC in human mPFC with electrocorticogram (ECoG) recording across a range of cognitive tasks. This may be because the PAC appeared between the theta and the high gamma oscillation (80–150 Hz) (Canolty et al., 2006), while such high frequency oscillation might not be detected with scalp EEG in our study. In addition, the enhanced theta-gamma coupling in STN was accompanied by elevated theta power during conflict processing while there was no significant correlation between them. Thus, both the theta amplitude and theta-gamma PAC contributed to conflict processing but they did not depend each other and may play complementary roles.

The current study not only revealed enhanced STN PAC during conflict processing but also demonstrated that faster responses are accompanied by stronger PACs. Similar behavior predictions have been reported before. In rodents, the strength of hippocampus theta-gamma coupling increased as the performance of a T-maze task increased (Tort et al., 2008), and stronger theta-gamma coupling in human fronto-parietal cortex predicted faster reaction times in a spatial-cuing task (Szczepanski et al., 2014). These studies provided evidence that PAC serves a functional role in the brain and no single frequency band is solely responsible for cognitive process, in accord with the notion that cognitive process is not a unitary function. STN has been proposed to operationalize “hold your horses” function by dynamically modulating decision thresholds in proportion to decision conflict (Frank

et al., 2007). The increased STN theta power has been considered as a mechanism in the adjustments of decision threshold (Cavanagh et al., 2011; Herz et al., 2016). According to our results, the STN may serve a "hold your horses" function during conflict by not only with increase in theta power but also with enhancement of theta-gamma coupling.

4.4. Co-occurrence of long-range phase synchronization and local PAC in fronto-subthalamic circuit

Our results revealed a combination of within- and between-frequency coupling in fronto-subthalamic circuit for conflict processing. It has been shown that high-frequency brain activity reflects local domains of processing, while low-frequency brain rhythms are dynamically entrained across distributed brain regions (Canolty and Knight, 2010), which means an inverse relation exists between the scale of integration and the frequency of interaction (Von Stein and Sarnthein, 2000). Hence, instead of establishing spatially restricted synchronization to areas directly within high-frequency bands, distant brain areas could indirectly coordinate high-frequency activity through the combination of long-distance, low-frequency phase synchronization and local cross-frequency PAC. Given the proposed role of mPFC in conflict monitoring, the control of mPFC over conflict related gamma activity in the STN may be achieved through the phase synchronization of theta activity between the two areas, combined with the local coordination of gamma activity within the STN via PAC (Fig. 7). Such combination did not mean the STN gamma activity was directly modulated by mPFC theta activity during conflict processing as we demonstrated no significant difference in mPFC-STN theta-gamma coupling between the conflict and non-conflict conditions. The reason may be because the mPFC and STN theta phases were far from perfectly synchronized as the average unnormalized mPFC-STN theta phase coherence for incongruent trials was relatively low at 0.29 ± 0.15 (mean ± SD). A combination of long-range phase synchronization and local PAC has been reported in human cortico-cortical interactions (Daume et al., 2017; Reinhart and Nguyen, 2019) and now demonstrated in human cortico-subcortical interactions by our data. To our knowledge, our study is the first to report direct evidence for such mechanism in fronto-subthalamic circuit for conflict processing.

Our data were recorded from PD patients who had undergone DBS surgery, thus our results may be affected by PD and may not represent normal functioning and corresponding neural activities (Geraedts et al., 2018; Hammond et al., 2007). However, recordings were made while patients were on their regular medications in an attempt to approximate normal physiological functioning as closely as possible. Moreover, both EEG and LFP recordings are subject to volume conduction of electrical signals. In order to mitigate this effect, we analyzed our data using a bipolar configuration of adjacent channels.

In conclusion, the current study demonstrated that mPFC-STN may coordinate their activities in slower rhythms to engage stimulus-related processing in faster rhythms via the combination of long-range, within-frequency phase synchronization and local cross-frequency phase amplitude coupling. Moreover, the enhanced STN theta-gamma coupling during conflict processing provides a novel mechanism by which the STN may operationalize its proposed "hold-your-horses" role.

Acknowledgment

This study was funded by the Canadian Institutes of Health Research (FDN 154292, ENG 173742), the Natural Science and Engineering Research Council of Canada (RGPIN-2020-04176) and the National Institute of Neurological Disorders and Stroke (NIH NS106822). K.Z was supported by a Canadian Institutes of Health Research postdoctoral fellowship (MFE-171317). N.M.D was supported by a Canadian Institutes of Health Research postdoctoral fellowship (MFE-164728).

References

Aron AR, Behrens TE, Smith S, Frank MJ, Poldrack RA, 2007. Triangulating a cognitive control network using diffusion-weighted Magnetic Resonance Imaging (MRI) and functional MRI. J. Neurosci 27, 3743–3752. [PubMed: 17409238]

Aron AR, Herz DM, Brown P, Forstmann BU, Zaghloul K, 2016. Frontosubthalamic circuits for control of action and cognition. J. Neurosci 36, 11489–11495. [PubMed: 27911752]

Aru J, Aru J, Priesemann V, Wibral M, Lana L, Pipa G, Singer W, Vicente R, 2015. Untangling cross-frequency coupling in neuroscience. Curr. Opin. Neurobiol 31, 51–61. [PubMed: 25212583]

Botvinick MM, 2007. Conflict monitoring and decision making:reconciling two perspectives on anterior cingulate function. Cogn. Affect. Behav. Neurosci 7, 356–366. [PubMed: 18189009]

Botvinick MM, Cohen JD, Carter CS, 2004. Conflict monitoring and anterior cingulate cortex: an update. Trends Cogn. Sci 8, 539–546. [PubMed: 15556023]

Brittain J-S, Watkins KE, Joundi RA, Ray NJ, Holland P, Green AL, Aziz TZ, Jenkinson N, 2012. A Role for the subthalamic nucleus in response inhibition during conflict. J. Neurosci 32, 13396–13401. [PubMed: 23015430]

Canavier CC, 2015. Phase-resetting as a tool of information transmission. Curr. Opin. Neurobiol 31, 206–213. [PubMed: 25529003]

Canolty RT, Edwards E, Dalal SS, Soltani M, Nagarajan SS, Kirsch HE, Berger MS, Barbare NM, Knight RT, 2006. High gamma power is phase-locked to theta oscillations in human neocortex. Science 313, 1626–1628. [PubMed: 16973878]

Canolty RT, Knight RT, 2010. The functional role of cross-frequency coupling. Trends Cogn. Sci 14, 506–515. [PubMed: 20932795]

Cardin JA, Carlén M, Meletis K, Knoblich U, Zhang F, Deisseroth K, Tsai L-H, Moore CI, 2009. Driving fast-spiking cells induces gamma rhythm and controls sensory responses. Nature 459, 663–667. [PubMed: 19396156]

Cavanagh JF, Frank MJ, 2014. Frontal theta as a mechanism for cognitive control. Trends Cogn. Sci 18, 414–421. [PubMed: 24835663]

Cavanagh JF, Wiecki TV, Cohen MX, Figueroa CM, Samanta J, Sherman SJ, Frank MJ, 2011. Subthalamic nucleus stimulation reverses mediofrontal influence over decision threshold. Nat. Neurosci 14, 1462–1467. [PubMed: 21946325]

Cavanagh JF, Zambrano-Vazquez L, Allen JJB, 2012. Theta lingua franca: A common mid-frontal substrate for action monitoring processes. Psychophysiology 49, 220–238. [PubMed: 22091878]

Chen W, De Hemptinne C, Miller AM, Lim DA, Larson PS, Starr PA, Chen W, De Hemptinne C, Miller AM, Leibbrand M, Little SJ, Lim DA, 2020. Prefrontal–subthalamic hyperdirect pathway modulates movement inhibition in humans. Neuron 1–10.

Cohen MX, 2014. A neural microcircuit for cognitive conflict detection and signaling. Trends Neurosci. 37, 480–490. [PubMed: 25034536]

Cohen MX, Cavanagh JF, 2011. Single-trial regression elucidates the role of prefrontal theta oscillations in response conflict. Front. Psychol 2, 1–12. [PubMed: 21713130]

Cohen MX, Elger CE, Fell J, 2009. Oscillatory activity and phase-amplitude coupling in the human medial frontal cortex during decision making. J. Cogn. Neurosci 21, 390–402. [PubMed: 18510444]

Cohen MX, Gulbinaite R, 2014. Five methodological challenges in cognitive electrophysiology. Neuroimage 85, 702–710. [PubMed: 23954489]

Daume J, Gruber T, Engel AK, Friese U, 2017. Phase-amplitude coupling and long-range phase synchronization reveal frontotemporal interactions during visual working memory. J. Neurosci 37, 313–322. [PubMed: 28077711]

Daume J, Wang P, Maye A, Zhang D, Engel AK, 2021. Non-rhythmic temporal prediction involves phase resets of low-frequency delta oscillations. Neuroimage 224, 117376. doi: 10.1016/j.neuroimage.2020.117376.

De Hemptinne C, Swann NC, Ostrem JL, Ryapolova-Webb ES, Luciano MS, Galifianakis NB, Starr PA, 2015. Therapeutic deep brain stimulation reduces cortical phase-amplitude coupling in Parkinson's disease. Nat. Neurosci 18, 779–786. [PubMed: 25867121]

DeLong MR, 1990. Primate models of movement disorders of basal ganglia origin. Trends Neurosci. 13, 281–285. [PubMed: 1695404]

Frank MJ, Samanta J, Moustafa AA, Sherman SJ, 2007. Hold your horses: impulsivity, deep brain stimulation, and medication in Parkinsonism. Science 318, 1309–1312. [PubMed: 17962524]

Fries P, 2015. Rhythms for cognition: communication through coherence. Neuron 88, 220–235. [PubMed: 26447583]

Fries P, 2005. A mechanism for cognitive dynamics: neuronal communication through neuronal coherence. Trends Cogn. Sci 9, 474–480. [PubMed: 16150631]

Geraedts VJ, Boon LI, Marinus J, Gouw AA, van Hilten JJ, Stam CJ, Tannemaat MR, Contarino MF, 2018. Clinical correlates of quantitative EEG in Parkinson disease: a systematic review. Neurology 91, 871–883. [PubMed: 30291182]

Ghahremani A, Aron AR, Udupa K, Saha U, Reddy D, Hutchison WD, Kalia SK, Hodaie M, Lozano AM, Chen R, 2018. Event-related deep brain stimulation of the subthalamic nucleus affects conflict processing. Ann. Neurol 84, 515–526. [PubMed: 30152889]

Hammond C, Bergman H, Brown P, 2007. Pathological synchronization in Parkinson's disease: networks, models and treatments. Trends Neurosci 30, 357–364. [PubMed: 17532060]

Helfrich RF, Knight RT, 2016. Oscillatory dynamics of prefrontal cognitive control. Trends Cogn. Sci 20, 916–930. [PubMed: 27743685]

Herz DM, Zavala BA, Bogacz R, Brown P, 2016. Neural correlates of decision thresholds in the human subthalamic nucleus. Curr. Biol 26, 916–920. [PubMed: 26996501]

Hyafil A, Giraud AL, Fontolan L, Gutkin B, 2015. Neural cross-frequency coupling: connecting architectures, mechanisms, and functions. Trends Neurosci. 38, 725–740. [PubMed: 26549886]

Jenkinson N, Kühn AA, Brown P, 2013. Gamma oscillations in the human basal ganglia. Exp. Neurol 245, 72–76. [PubMed: 22841500]

Kelley R, Flouty O, Emmons EB, Kim Y, Kingyon J, Wessel JR, Oya H, Greenlee JD, Narayanan NS, 2018. A human prefrontal-subthalamic circuit for cognitive control. Brain 141, 205–216. [PubMed: 29190362]

Lachaux J-P, Lutz A, Rudrauf D, Cosmelli D, Le Van Quyen M, Martinerie J, Varela F, 2002. Estimating the time-course of coherence between single-trial brain signals: an introduction to wavelet coherence. Neurophysiol. Clin. Neurophysiol 32, 157–174.

Lopez-Azcarate J, Tainta M, Rodriguez-Oroz MC, Valencia M, Gonzalez R, Guridi J, Iriarte J, Obeso JA, Artieda J, Alegre M, 2010. Coupling between Beta and high-frequency activity in the human subthalamic nucleus may be a pathophysiological mechanism in Parkinson's disease. J. Neurosci 30, 6667–6677. [PubMed: 20463229]

Maris E, Oostenveld R, 2007. Nonparametric statistical testing of EEG- and MEG-data. J. Neurosci. Methods 164, 177–190. [PubMed: 17517438]

Mink JW, 1996. The basal ganglia: focused selection and inhibition of competing motor programs. Prog. Neurobiol.

Narayanan NS, Cavanagh JF, Frank MJ, Laubach M, 2013. Common medial frontal mechanisms of adaptive control in humans and rodents. Nat. Neurosci 16, 1888–1895. [PubMed: 24141310]

Nolte G, Bai O, Wheaton L, Mari Z, Vorbach S, Hallett M, 2004. Identifying true brain interaction from EEG data using the imaginary part of coherency. Clin. Neurophysiol 115, 2292–2307. [PubMed: 15351371]

Oostenveld R, Fries P, Maris E, Schoffelen JM, 2011. FieldTrip: open source software for advanced analysis of MEG, EEG, and invasive electrophysiological data. Comput. Intell. Neurosci 2011.

Reinhart RMG, Nguyen JA, 2019. Working memory revived in older adults by synchronizing rhythmic brain circuits. Nat. Neurosci 22, 820–827. [PubMed: 30962628]

Rodriguez-Oroz MC, López-Azcárate J, Garcia-Garcia D, Alegre M, Toledo J, Valencia M, Guridi J, Artieda J, Obeso JA, 2011. Involvement of the subthalamic nucleus in impulse control disorders associated with Parkinson's disease. Brain 134, 36–49. [PubMed: 21059746]

Swann NC, De Hemptinne C, Aron AR, Ostrem JL, Knight RT, Starr PA, 2015. Elevated synchrony in Parkinson disease detected with electroencephalography. Ann. Neurol.

Sweeney-Reed CM, Zaehle T, Voges J, Schmitt FC, Buentjen L, Kopitzki K, Esslinger C, Hinrichs H, Heinze HJ, Knight RT, Richardson-Klavehn A, 2014. Corticothalamic phase synchrony and cross-frequency coupling predict human memory formation. Elife 3, e05352. [PubMed: 25535839]

Szczepanski SM, Crone NE, Kuperman RA, Auguste KI, Parvizi J, Knight RT, 2014. Dynamic changes in phase-amplitude coupling facilitate spatial attention control in fronto-parietal cortex. PLoS Biol. 12.

Tort ABL, Komorowski RW, Manns JR, Kopell NJ, Eichenbaum H, 2009. Theta-gamma coupling increases during the learning of item-context associations. Proc. Natl. Acad. Sci. U. S. A 106, 20942–20947. [PubMed: 19934062]

Tort ABL, Kramer MA, Thorn C, Gibson DJ, Kubota Y, Graybiel AM, Kopell NJ, 2008. Dynamic cross-frequency couplings of local field potential oscillations in rat striatum and hippocampus during performance of a T-maze task. Proc. Natl. Acad. Sci. U. S. A 105, 20517–20522. [PubMed: 19074268]

Vinck M, van Wingerden M, Womelsdorf T, Fries P, Pennartz CMA, 2010. The pairwise phase consistency: a bias-free measure of rhythmic neuronal synchronization. Neuroimage 51, 112–122. [PubMed: 20114076]

von Nicolai C, Engler G, Sharott A, Engel AK, Moll CK, Siegel M, 2014. Corticostriatal coordination through coherent phase-amplitude coupling. J. Neurosci 34, 5938–5948. [PubMed: 24760853]

Von Stein A, Sarnthein J, 2000. Different frequencies for different scales of cortical integration: from local gamma to long range alpha/theta synchronization. Int. J. Psychophysiol 38, 301–313. [PubMed: 11102669]

Wessel JR, Ghahremani A, Udupa K, Saha U, Kalia SK, Hodaie M, Lozano AM, Aron AR, Chen R, 2016a. Stop-related subthalamic beta activity indexes global motor suppression in Parkinson's disease. Mov. Disord 31, 1846–1853. [PubMed: 27474845]

Wessel JR, Jenkinson N, Brittain JS, Voets SHEM, Aziz TZ, Aron AR, 2016b. Surprise disrupts cognition via a fronto-basal ganglia suppressive mechanism. Nat. Commun 7, 1–10.

Womelsdorf T, Schoffelen JM, Oostenveld R, Singer W, Desimone R, Engel AK, Fries P, 2007. Modulation of neuronal interactions through neuronal synchronization. Science 316, 1609–1612. [PubMed: 17569862]

Zavala B, Brittain J-S, Jenkinson N, Ashkan K, Foltynie T, Limousin P, Zrinzo L, Green AL, Aziz T, Zaghloul K, Brown P, 2013. Subthalamic nucleus local field potential activity during the eriksen flanker task reveals a novel role for theta phase during conflict monitoring. J. Neurosci 33, 14758–14766. [PubMed: 24027276]

Zavala B, Jang A, Trotta M, Lungu CI, Brown P, Zaghloul KA, 2018. Cognitive control involves theta power within trials and beta power across trials in the prefrontal-subthalamic network. Brain 141, 3361–3376. [PubMed: 30358821]

Zavala B, Tan H, Ashkan K, Foltynie T, Limousin P, Zrinzo L, Zaghloul K, Brown P, 2016. Human subthalamic nucleus-medial frontal cortex theta phase coherence is involved in conflict and error related cortical monitoring. Neuroimage 137, 178–187. [PubMed: 27181763]

Zavala B, Zaghloul K, Brown P, 2015. The subthalamic nucleus, oscillations, and conflict. Mov. Disord 30, 328–338. [PubMed: 25688872]

Zavala BA, Tan H, Little S, Ashkan K, Hariz M, Foltynie T, Zrinzo L, Zaghloul KA, Brown P, 2014. Midline frontal cortex low-frequency activity drives subthalamic nucleus oscillations during conflict. J. Neurosci 34, 7322–7333. [PubMed: 24849364]

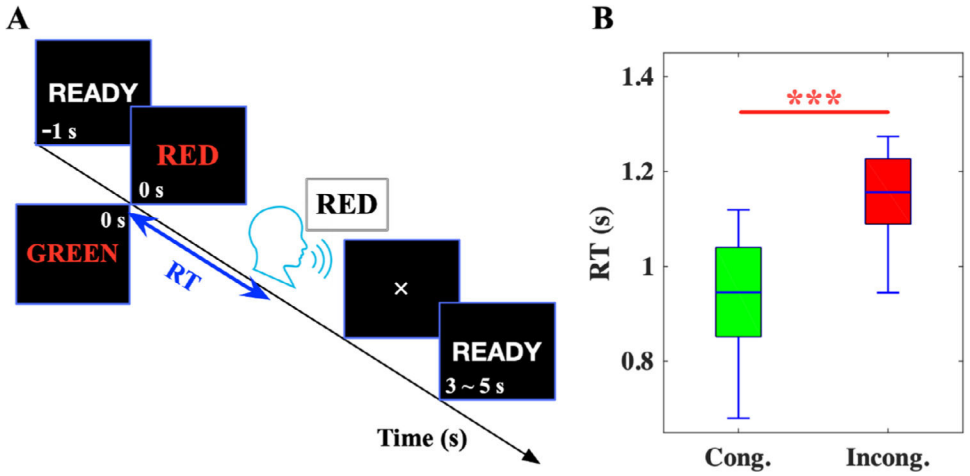

Fig. 1.

Stroop task and Stroop effect. (A) Stroop task. Each trial begins with a READY cue displayed for 1 s, after which a color word appears on the screen. Subject should respond as quickly with the ink color of the words and ignore their meaning. As illustrated, the subject would speak 'red' whether the word is 'RED' or 'GREEN'. A 1:1 ratio of incongruent to congruent trials was used in this study. (B) Box plot showing the Stroop effect. In each box, center line indicates the median, the box edges are the 25th and 75th percentiles, and the whiskers extend to the most extreme data points not considered outliers (1.5 × the interquartile range). The reaction times for the congruent (green) trials were significantly shorter than those for the incongruent (red) trials. *** denotes $p < 0.001$.

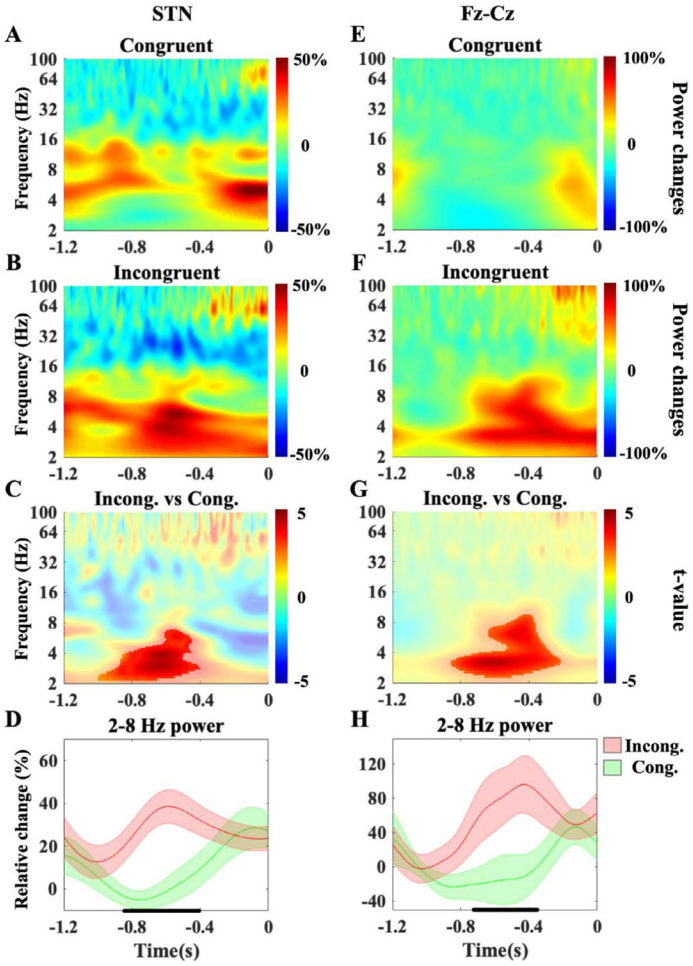

Fig. 2.

Response-aligned spectral power changes in STN LFP and mPFC EEG. A to D are spectral power changes in STN LFP. (A) and (B) are group mean spectral power for all congruent (Cong.) and incongruent trials (Incong). (C) Significant differences in spectral power between congruent and incongruent trials are masked ($p < 0.05$ after multiple correction). (D) Response-aligned theta band (2–8 Hz) average power time series (mean ± SEM) for congruent (green) and incongruent (red) trials. The times with significant difference between the two conditions are marked by the black bar ($p < 0.05$ corrected for multiple comparisons). E to H are same as A to D but show spectral power changes in mPFC EEG.

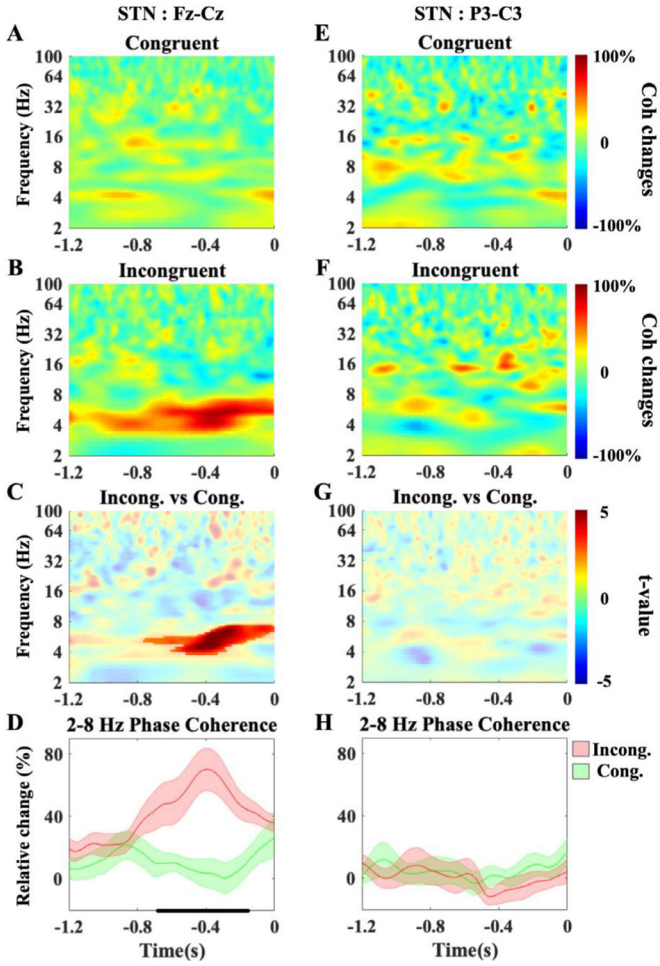

Fig. 3.

Response-aligned phase coherence (Coh) between STN LFP and scalp EEG. A to D show phase coherence between STN LFP and mPFC EEG. (A) and (B) are mean phase coherence for all congruent and incongruent trials. (C) Shows the time-frequencies for significantly higher phase coherence when incongruent trials were compared to congruent trials (masked at $p < 0.05$ corrected for multiple comparisons). (D) Response-aligned average phase coherence time series (mean ± SEM) in the theta band (2–8 Hz) for congruent (green) and incongruent (red) trials. The times with significant difference between the two conditions are marked by black bar ($p < 0.05$ corrected for multiple comparisons). E to H are same as A to D but show phase coherence between STN LFP and left parietal EEG.

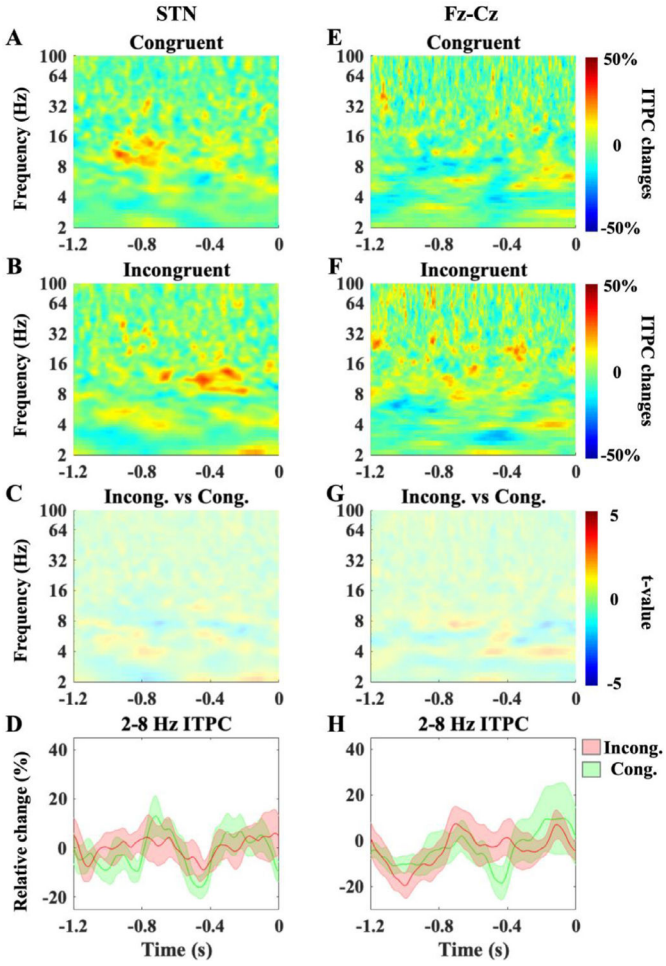

Fig. 4.

Response-aligned inter-trial phase clustering (ITPC) in STN LFP and mPFC EEG. A to D are ITPC in STN LFP. (A) and (B) are mean ITPC for congruent (Cong.) and incongruent (Incog.) trials. (C) shows no significant difference in time-frequency ITPC between incongruent and congruent trials. (D) Response-aligned theta band (2–8 Hz) mean ITPC time series (mean ± SEM) for congruent (green) and incongruent (red) trials. There was no significant difference in the time series of theta ITPC between the two conditions. E to H are same as A to D but show ITPC in mPFC EEG.

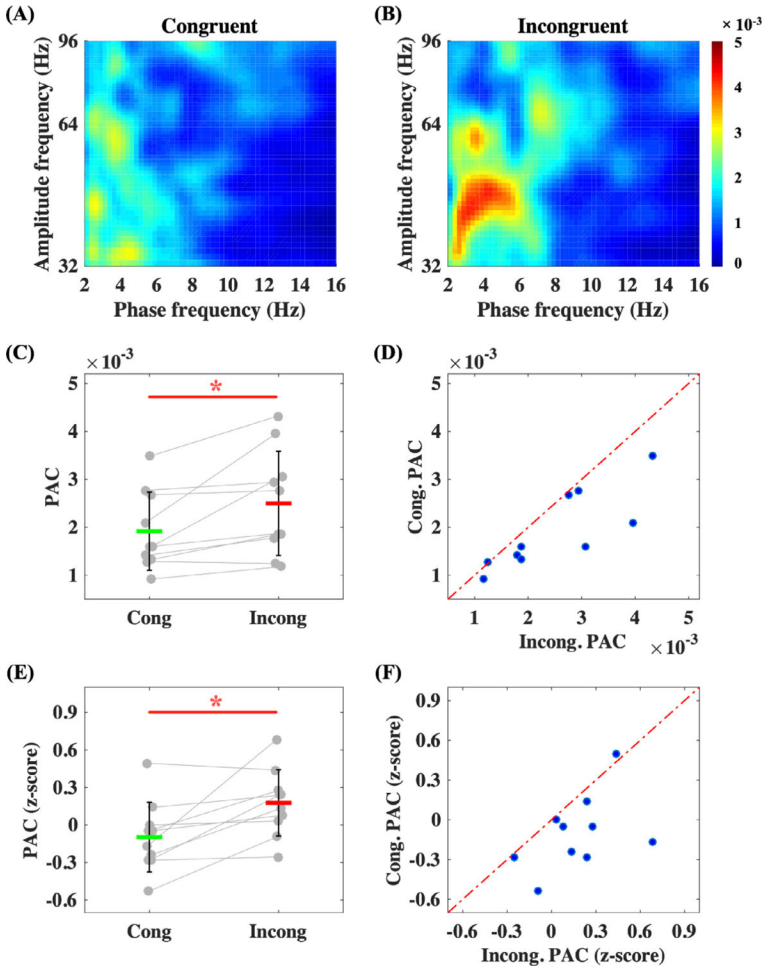

Fig. 5.

Phase-amplitude coupling (PAC) in the STN. (A) and (B) show the mean group phase-to-amplitude comodulograms across all subjects for congruent and incongruent trials. Frequency is given in a log scale in the vertical axis. (C) Bar plot showing group average of PAC values over theta phase frequencies (2–8 Hz) and gamma amplitude frequencies (32–64 Hz) for congruent (green) and incongruent (red) trials. Error bars represent standard deviation. Each gray line depicts a single subject. (D) Individual subject's PAC values for congruent and incongruent trials. Each circle represents data from a single subject with PAC calculated separately for incongruent trials (*x* axis) and congruent trials (*y* axis). (E) and (F) are the bar plot and individual plot for z-score of raw PAC values. Both raw theta-gamma PACs and their z-score for incongruent trials were significantly stronger than for congruent trials. In most subjects, STN theta-gamma coupling were higher for incongruent than congruent trials. * represents $p < 0.05$.

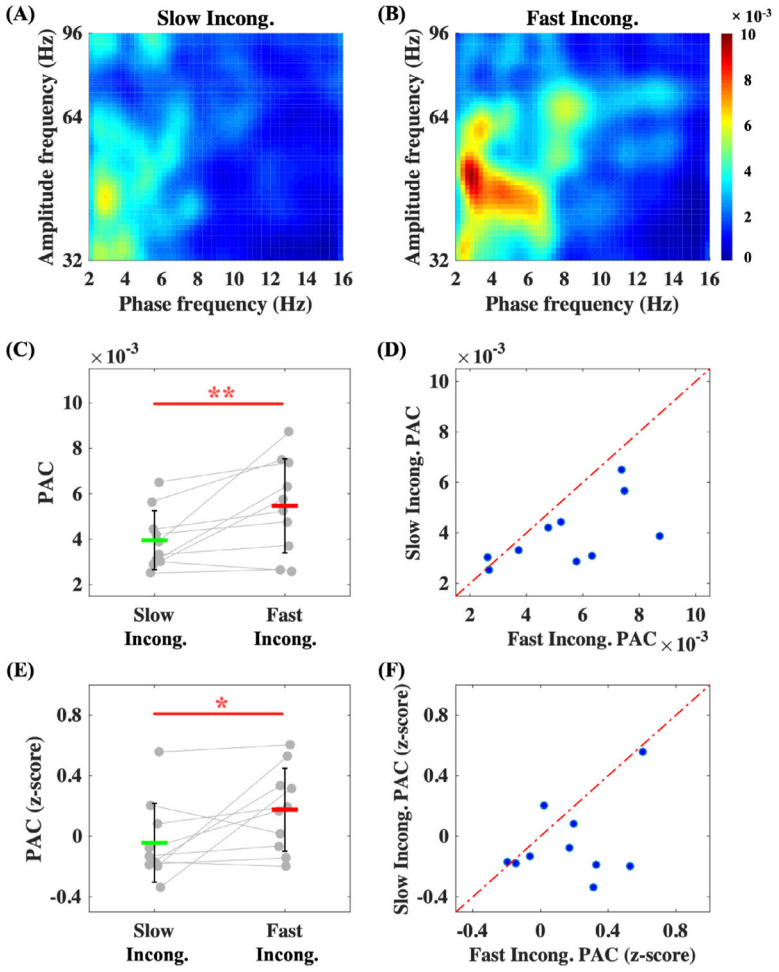

Fig. 6.

Phase-amplitude coupling (PAC) in STN for slow versus fast incongruent trials. (A) and (B) show the mean group phase-to-amplitude comodulograms across all subjects for slow incongruent and fast incongruent trials. Frequency is given in a log axis in the vertical axis. (C) Bar plot showing group average of PAC values over theta phase frequencies (2–8 Hz) and gamma amplitude frequencies (32–64 Hz) for slow incongruent (green) and fast incongruent (red) trials. Error bars represent standard deviation. Each gray line depicts a single subject. (D) Individual subject's PAC values for slow incongruent and fast incongruent trials. Each circle represent data from a single subject with PAC calculated separately for fast incongruent trials (x axis) and slow incongruent trials (y axis). (E) and (F) are the bar plot and individual plot for z-score of raw PAC values. Both raw theta-gamma PACs and their z-score for fast incongruent trials were significantly stronger than for slow congruent trials. In most subjects, STN theta-gamma coupling were higher for fast incongruent than slow incongruent trials. * and ** represent $p < 0.05$ and $p < 0.01$.

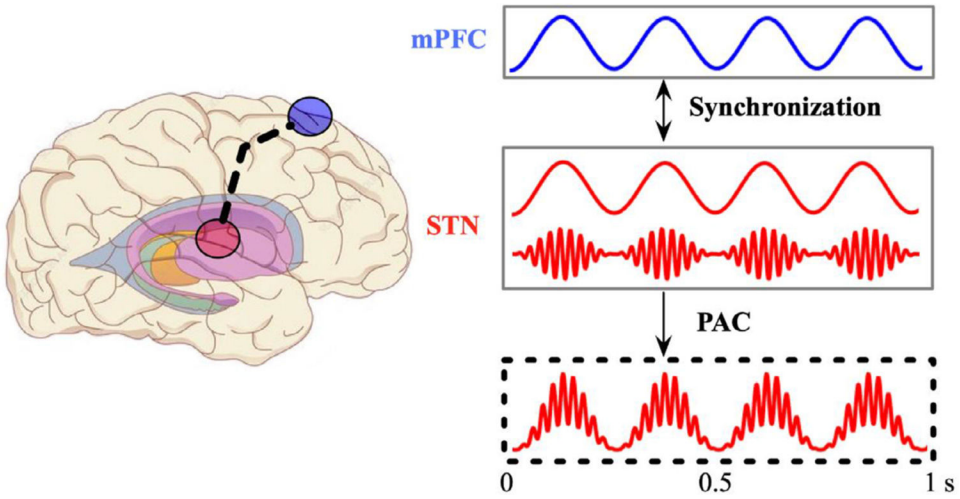

Fig. 7.

Schematic illustration of the combination of long-range, within-frequency phase synchronization and local cross-frequency PAC in the fronto-subthalamic circuit. The dashed line in the left represents the increased theta phase synchronization between the mPFC and the STN during conflict processing. The dash box in the bottom right depicts that conflict related gamma bursts prefer the peak of the theta activity in the STN, indicating the gamma amplitudes are modulated by the theta activity in the STN. Taken together, the mPFC modulates the gamma activities in the STN through phase synchronization of theta activity between the two areas, combined with the local theta-gamma PAC within the STN.